



Reaction chain modeling of denitrification reactions during a push–pull test



A. Boisson^{*}, P. de Anna¹, O. Bour, T. Le Borgne, T. Labasque, L. Aquilina

Géosciences Rennes-OSUR, UMR CNRS 6118, University of Rennes 1, France

ARTICLE INFO

Article history:

Received 3 April 2012

Received in revised form 29 January 2013

Accepted 8 February 2013

Available online 24 February 2013

Keywords:

Reaction chain modeling

Push–pull test

Denitrification

Nitrous oxide

ABSTRACT

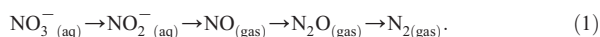
Field quantitative estimation of reaction kinetics is required to enhance our understanding of biogeochemical reactions in aquifers. We extended the analytical solution developed by Haggerty et al. (1998) to model an entire 1st order reaction chain and estimate the kinetic parameters for each reaction step of the denitrification process. We then assessed the ability of this reaction chain to model biogeochemical reactions by comparing it with experimental results from a push–pull test in a fractured crystalline aquifer (Ploemeur, French Brittany). Nitrates were used as the reactive tracer, since denitrification involves the sequential reduction of nitrates to nitrogen gas through a chain reaction ($\text{NO}_3^- \rightarrow \text{NO}_2^- \rightarrow \text{NO} \rightarrow \text{N}_2\text{O} \rightarrow \text{N}_2$) under anaerobic conditions. The kinetics of nitrate consumption and by-product formation (NO_2^- , N_2O) during autotrophic denitrification were quantified by using a reactive tracer (NO_3^-) and a non-reactive tracer (Br^-). The formation of reaction by-products (NO_2^- , N_2O , N_2) has not been previously considered using a reaction chain approach. Comparison of Br^- and NO_3^- breakthrough curves showed that 10% of the injected NO_3^- molar mass was transformed during the 12 h experiment (2% into NO_2^- , 1% into N_2O and the rest into N_2 and NO). Similar results, but with slower kinetics, were obtained from laboratory experiments in reactors. The good agreement between the model and the field data shows that the complete denitrification process can be efficiently modeled as a sequence of first order reactions. The 1st order kinetics coefficients obtained through modeling were as follows: $k_1 = 0.023 \text{ h}^{-1}$, $k_2 = 0.59 \text{ h}^{-1}$, $k_3 = 16 \text{ h}^{-1}$, and $k_4 = 5.5 \text{ h}^{-1}$. A next step will be to assess the variability of field reactivity using the methodology developed for modeling push–pull tracer tests.

© 2013 Elsevier B.V. All rights reserved.

1. Introduction

Predicting reactive transport remains a challenge in hydrogeology. Within this field, the reduction of nitrates by denitrification (Korom, 1992; Mariotti, 1986) is common in soil and groundwater since the use of fertilizers in modern agriculture has led to high nitrate concentrations in aquifers. Understanding the kinetics of denitrification is important for determining the attenuation of nitrate concentrations in aquifers and for management. Denitrification is the sequential reduction of

nitrates to nitrogen gas which occurs under anaerobic conditions and can be represented as the following chain reaction (Betlach and Tiedje, 1981):



Various studies involving batch experiments and column experiments have been used to quantify the reaction kinetics at the laboratory scale (Amirbahman et al., 2003; Postma and Appelo, 2000; Vongunten and Zobrist, 1993). However, due to the difficulties of reproducing natural conditions in laboratory experiments as well as the scale effects related to physical heterogeneity (Dentz et al., 2011), field measurements are required to quantify reactive transport at the field scale. Thus different experimental setups have been developed to quantify

^{*} Corresponding author at: BRGM, D3E/NRE, Indo-French Centre for Groundwater Research, Hyderabad, India.

E-mail address: a.boisson@brgm.fr (A. Boisson).

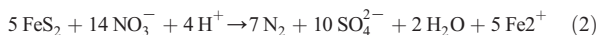
¹ Now at Massachusetts Institute of Technology, MA, USA.

denitrification reactions in the field using borehole networks (McAllister and Chiang, 1994), isotopic characterization (Otero et al., 2009; Pauwels et al., 2010), tracer tests (Pauwels et al., 1998) and push–pull tests (Addy et al., 2002; Istok et al., 1997; Kim et al., 2005; McGuire et al., 2002).

However, these reactions are often studied on very small time scales (hours in the case of push–pull tests). In experiments of short duration and under dynamic conditions, the reactions are often incomplete and lead to the formation of by-products, such as nitrites and nitrous oxide in the case of nitrate reduction. Knowledge of the kinetics of nitrate consumption and by-product production is essential to better understand these biogeochemical reactions.

To tackle this problem we developed a model of the entire denitrification chain reaction and compared it with field measurements. Our aim was to provide a framework which allowed assessment of the complete chain reaction. Nitrate degradation in natural media has already been modeled as a first order degradation process (Knowles, 1982; Pauwels et al., 1998). Analytical solutions for first order chain reactions have already been developed but generally require knowledge of the transport properties of the medium (Bauer et al., 2001; Quezada et al., 2004). However, as suggested by Haggerty et al. (1998), the first order reaction rate can be determined from push–pull tests using a simplified analytical solution without direct knowledge of the physical properties of the aquifer. Such a solution is very useful in the case of push–pull tests since this kind of experiment does not require knowledge of physical parameters such as porosity and limited information about transport is available without further experiments. Following Haggerty et al. (1998), we developed a semi-analytical solution to model nitrate reduction and by-product formation through a first order chain reaction. Field and laboratory experiments were then conducted to assess its reliability for predicting by-product formation.

Most field studies have been focused on aquifers contaminated by hydrocarbons i.e. heterotrophic denitrification since the hydrocarbons are used as carbon sources (Cozzarelli et al., 1999; Schroth et al., 1998; Vandenbohede et al., 2008). However denitrification may also have an important role in zones of intensive agriculture with low organic carbon contents, as in the crystalline aquifers of French Brittany (Aquilina et al., 2012; Tarits et al., 2006). In the case of the Ploemeur aquifer (Brittany, France), it has been shown that due to the very low carbon content, heterotrophic denitrification is negligible but that nitrate reduction occurs via microbial autotrophic denitrification with pyrite following Eqs. (2) & (3) (Tarits et al., 2006):



Although this reaction can occur under abiotic conditions, it is very slow under such conditions (Weber et al., 2001). In aquifers the reaction rate is controlled in part by the repartition and development of microbial populations (Philippot et al., 2009). Autotrophic denitrification has been studied in various countries of western Europe, namely in sandy aquifers in the Netherlands (Miotliński, 2008; Postma et al., 1991; Zhang et al., 2009, 2012) or Spain (Otero et al., 2009), in limestone aquifers in France (Mariotti et al., 1988) or England (Hiscock et al.,

2003; Muhlherr and Hiscock, 1998), and in gravel and sandy aquifers in Germany (Fukada et al., 2003; Weymann et al., 2008) but very few studies have been conducted to assess the kinetics of autotrophic denitrification in fractured crystalline media (Pauwels et al., 1998; Tarits et al., 2006). Therefore, our second objective was to quantify autotrophic denitrification in a fractured crystalline aquifer. This was done through laboratory tests and in situ push–pull test experiments. In highly heterogeneous media it is clear that push–pull tests can only provide a local evaluation of the reaction kinetics. However, compared to classical tracer tests, they allow denitrification to be measured on a field scale with good tracer recovery.

Among the various by-products (Eq. (1)), the formation of nitrous oxide, a major greenhouse gas, has been largely studied in aquifers and sediments (Mosier et al., 1998). Measurements of denitrification, including those of the by-products, are difficult to obtain as the gases produced, mainly N_2 and to a lesser extent N_2O , are already present in the natural environment. Different methods have been used to quantify this production, ranging from laboratory experiments (Laverman et al., 2010; Silvennoinen et al., 2008) to the aquifer scale (Hiscock et al., 2003; Muhlherr and Hiscock, 1998; Weymann et al., 2008). These studies provided reliable results but few of them were able to quantify nitrous oxide formation on the field scale from an accurately known input of nitrate into the system (Addy et al., 2002; Kim et al., 2005; Weymann et al., 2008). Moreover, to our knowledge, no field scale experiment has been carried out to quantify the production of nitrous oxide from autotrophic denitrification, which was the third objective of this study.

In the first section, we present the experimental setups, and the modeling approach developed. We then describe the results obtained in the field and the laboratory, which were used in the model to determine kinetic parameters.

2. Material and methods

2.1. Site presentation

The crystalline rock aquifer of Ploemeur is the main source of tap water for the town of Ploemeur (18 000 hab) with an annual water production rate of about $1.10^6 \text{ m}^3/\text{year}$ since 1991. The pumping site and the productive boreholes are located at the contact zone between the Ploemeur granites and the overlying micaschists (Fig. 1) (Touchard, 1999). This contact zone, which dips moderately to the north (around 30°) consists of alternating deformed granitic sheets (including mylonites and pegmatite-bearing breccias) and enclaves of micaschists, pegmatite and aplite dykes, as well as quartz veins (Ruelleu et al., 2010). Flow in this geological media is highly heterogeneous and localized in a limited number of fractures at depths ranging between 40 and 150 m within the pumping site (Le Borgne et al., 2006). Deformation and permeability may be locally enhanced by a steeply dipping fault striking North 20° , with combined dextral strike-slip and normal components (Fig. 1). It should be noted that boreholes drilled only in the Ploemeur granite (south of the contact zone) or only in the micaschists (north of the contact zone) were mostly unproductive.

About 60% of the watershed surface is devoted to agriculture, which results in nitrate concentrations that vary between 40 and 120 mg/L in most of the boreholes around the pumping site. However, the nitrate concentrations in the pumping well

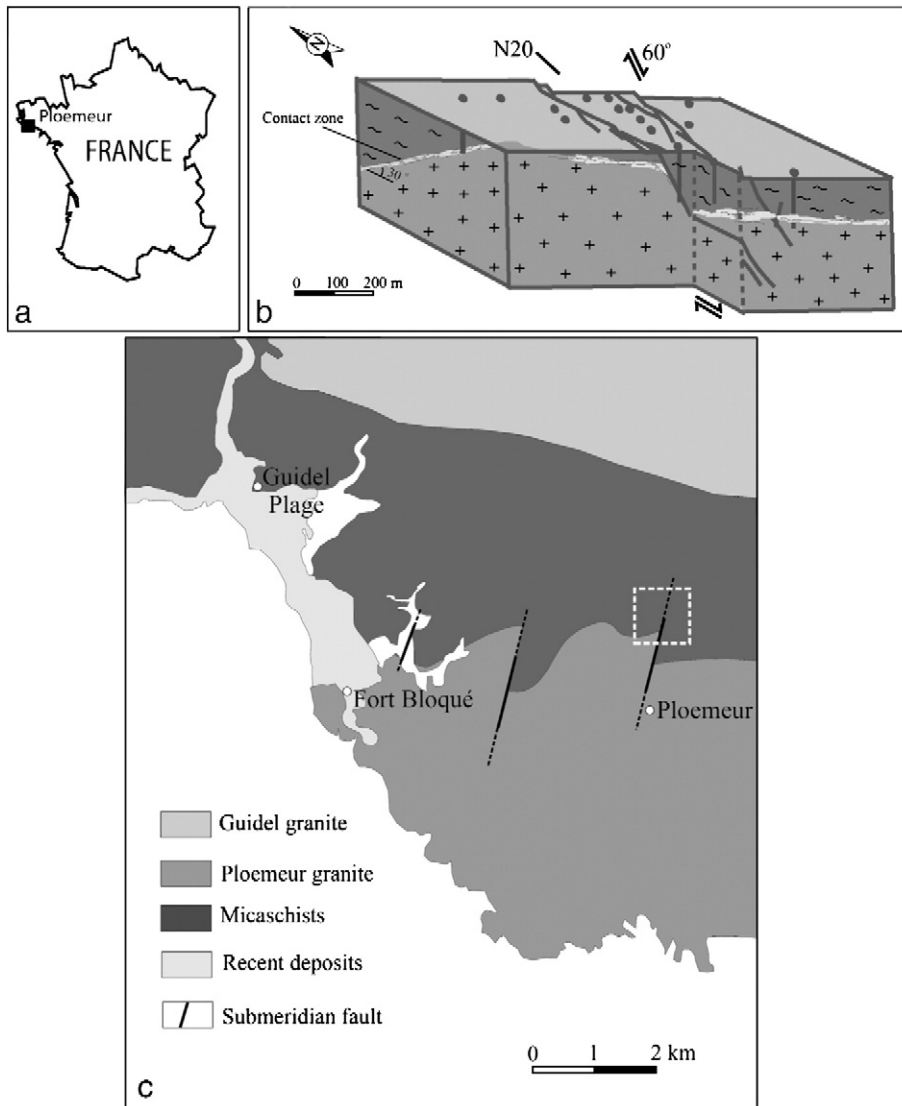


Fig. 1. Ploemeur site representation; a) Location of the site, b) schematic 3D diagram of the Ploemeur pumping site showing the regional contact dipping toward the North and the N20 dextral normal fault along which many boreholes were drilled (modified from Le Borgne et al., 2006), c) Synthetic geological map of Ploemeur area (modified from Ruellet et al., 2010). White square shows the pumping site location.

remained below 5 mg/L. Due to pumping within the area (Le Borgne et al., 2006; Leray et al., 2012), a mixing of different chemical water groups may also occur in the Ploemeur site (Fig. 1b). Previous studies (Tarits et al., 2006) revealed the occurrence of a microbial autotrophic denitrification reaction related to fractures containing pyrite but the reaction kinetics have not been quantified.

To avoid any influence from the pumping site and any contamination of the pumped water, the push–pull test was carried out at an experimental site located 3 km away in the same geologic and hydrogeologic conditions (Fig. 1c). This secondary site consisted of four boreholes 70 to 100 m deep. All four boreholes were located within a very small area (12×3 m) to facilitate the tracer and push–pull tests. This site is very similar to another nearby experimental site that

has been described in detail in Le Borgne et al. (2007). The lithologies consist mainly of fractured and deformed micaschists, but pegmatites and aplites may be encountered locally. Although the boreholes are very close to each other, the site is highly heterogeneous with variable transmissivity from the different boreholes (mean transmissivity 2.10^{-4} m/s). Water level measurements did not reveal any gradient between the different boreholes. The low gradient and low permeability imply that flow between the different boreholes is very slow. The site was characterized by performing a set of pumping tests within the different screened boreholes and by carrying out single and cross borehole flowmeter tests using an impeller and a heatpulse flowmeter (Molz et al., 1994; Paillet, 1998). In addition, a multi-parameter probe TROLL 9500 (WinSitu) was used for temperature, conductivity, dissolved oxygen, Eh and

pH logging. Water chemistry measurements, including CFC analysis, were also obtained from the different boreholes at different depths and times.

The F26 borehole, which is characterized by a single fracture zone at 64 m depth, was selected for the push–pull test. The concentration of dissolved oxygen in the entire water column was below 250 $\mu\text{g/L}$ (probe detection limit). No nitrates or nitrites were observed in this borehole before the experiment. Continuous monitoring of the Ploemeur site (de Dreuzy et al., 2006; Tarits et al., 2006) revealed that this borehole was characterized by a very low NO_3^- concentration with the occasional occurrence of NO_2^- whereas the NO_3^- concentrations in some surrounding boreholes were maintained at around 40 mg/L. This indicates that NO_3^- reduction occurs naturally in the aquifer in the vicinity of this well.

2.2. Push–pull test design

A push–pull test consists of the injection of a known tracer solution in a single monitoring well followed by the extraction of the solution mixed with groundwater from the same well (Becker and Shapiro, 2003; Gouze et al., 2008; Haggerty et al., 2001; Istok et al., 1997; Le Borgne and Gouze, 2008; Meigs and Beauheim, 2001; Tsang, 1995). This push–pull method does not provide direct information about medium parameters such as porosity or the water rock interaction surface. Indeed, porosity and dispersivity cannot be determined from a push–pull test as the flow field is reversed in the middle of the experiment (Altman et al., 2002; Gouze et al., 2008; Haggerty et al., 2001). The breakthrough curve obtained during a push–pull experiment is controlled by irreversible dispersion which includes i) diffusion and its interaction with small-scale heterogeneities, ii) fracture matrix mass transfer and iii) mixing and reactivity (Le Borgne and Gouze, 2008).

The tracer solution was composed of 1425 mg/L Br^- (KBr, Fisher scientific – Laboratory reagent grade) and 2030 mg/L NO_3^- (NaNO_3 , Fisher scientific – Analytical reagent grade). The tracer solution was injected at a flow rate of 1 m^3/h for 15 min followed by a 55 min injection of water pumped from another borehole containing no nitrate or nitrite and with an oxygen concentration below 0.5 mg/L. These conditions were required to ensure the anaerobic conditions necessary for denitrification. We also checked that pumping in the borehole did not influence the water levels and flow conditions in the injection borehole. A resting time of 70 min was respected to allow tracer diffusion in the medium before back-pumping the tracer solution for 10 h. This procedure led to a maximum residence time of about 12 h for the tracer solution within the aquifer.

2.3. Borehole monitoring

The investigated borehole (F26) was 220 mm in diameter and screened from 45 to 79 m. The water level was at 3.9 m bgs. The injection was done at 64 m depth within the fractured zone. A multi-parameter probe TROLL 9500 (WinSitu), located at 50 m depth in the borehole, was used to measure O_2 , Eh, pH, conductivity and temperature. A borehole spectrophotometer (SCAN Spectrolyser), located at 55 m depth, allowed in situ continuous monitoring of the nitrate concentrations within the borehole between the pump and the flow zone. Water sampling

and chemical analyses of the pumped water were also carried out. The spectrophotometer had been developed for in situ borehole monitoring to a depth of 100 m. A specific calibration curve was determined. The pump (Grundfos MP1) used for tracer recovery was located at 40 m depth and the pumping rate was 1 m^3/h , similar to the injection rate. Since no fractures are present between 40 and 64 m depth difference between injection and recovery depth does not affect significantly the breakthrough curves. In addition, a pressure sensor (STS DLN 70) was placed at 10 meter depth in the injection borehole and in nearby boreholes.

2.4. Laboratory experiments: reactors

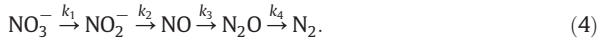
To compare our field results with those of laboratory experiments, the reaction was also assessed using batch reactors. These experiments were conducted in order to 1) assess the reaction in a non-dynamic and controlled medium, and 2) to compare laboratory kinetics with field results as few data were available. The reactors were filled with crushed granite (200 g, average size 0.6 mm) and untreated site water (400 mL) pumped from the injection well F26. As there was no poisoning, the microbial population naturally present in the water was expected to develop and to catalyze the reaction. Rocks were collected from core drilling of a borehole (at 60 m depth) located on the Ploemeur site 3 km away and crushed in the laboratory. Previous laboratory experiments involving samples of either granite or micaschist had given similar results in terms of reactivity and reaction kinetics. The low oxygen concentration (below 0.4 mg/L) in the water in the batch reactors was kept constant. The reactors consisted of 500 ml glass bottles closed with a plastic septum to allow sampling with a syringe. The bottles were purged with argon and kept under an argon atmosphere (gas headspace of 100 mL). A nitrate solution made from NaNO_3 powder (Fisher Scientific – Laboratory reagent grade) was injected to obtain an initial concentration of 37.5 mg/L in the reactor at the beginning of the experiment. The reactors were set up in triplicate and no relevant differences were observed between replicates. The reactors were analyzed for anions once a day and every two days for cations, organic and inorganic carbon. Gases (N_2O) were not measured due to the large volume needed for the analyses (500 mL). The experiments were run for 815 h.

2.5. Analytical methods

Before analysis, the anion, carbon and cation samples were filtered through a 0.2 μm Sartorius filter. The major anions (NO_3^- , Br^- , SO_4^{2-} , Cl^- , F^-) were analyzed using a Dionex DX 120 ion chromatograph. Organic and inorganic carbons were analyzed using a Shimadzu 5050A Total Organic Carbon analyzer (detection limit 400 ppb). The volume required for the analyses was 5 mL. The uncertainty for the anion measurements was 4%. Cations were analyzed by ICPMS (HP 4500) after acidification with nitric acid. Gases were obtained by headspace equilibrium, extraction and analyzed by $\mu\text{GC}/\text{TCD}$ (Agilent Micro GC3000 (SRA Instruments)). This method and the use of large volumes (500 mL) for the analyses allowed an uncertainty of 5% for the nitrogen gases (N_2O ; N_2).

2.6. Model development

The different reaction coefficients and the consistency of nitrate consumption and by-product formation were then estimated by testing the applicability of a model based on the following chain of 1st order reactions:



This model of chain kinetics was based on the analysis presented by Haggerty et al. (1998) for quantifying reactive push–pull tests. This reaction can be considered as irreversible under the studied conditions with very low oxygen content. The main advantages of the model were that: i) it allowed estimation of the reaction rate coefficient; ii) it was not dependent on the aquifer parameters since breakthrough curves do not depend on porosity or permeability and iii) it did not require a use of solutions for flow and transport (numerical or analytical). Two basic hypotheses were assumed. All the injected chemicals were locally well mixed and the retardation factors were the same for all tracers in the push–pull test.

The breakthrough curve of the conservative tracer concentration provides an estimate of the dilution of the injected solutions. The relative concentrations of the conservative and reactive tracer are given by:

$$\frac{C_{\text{react}}(t)}{C_{\text{react}}^0} = \frac{C_{\text{cons}}(t)e^{-k_1 t}}{C_{\text{cons}}^0} \quad (5)$$

where C_{react}^0 and C_{cons}^0 are the initial concentrations of the reactive and the conservative tracers injected in the well; and $C_{\text{react}}(t)$ and $C_{\text{cons}}(t)$ are the concentrations of reactive and conservative tracers that are measured during the extraction phase (Jury and Roth, 1990). Since the chain reaction also takes place during the injection phase, this effect also needs to be taken into account. For an injection time t_{inj} at a constant injection flow rate Q_{inj} , the nitrate concentration after the injection is given by:

$$C_{\text{NO}_3}(t) = \frac{C_{\text{NO}_3}^0}{C_{\text{Br}}^0} C_{\text{Br}}(t) \frac{1 - e^{-k_1 t_{\text{inj}}}}{k_1 t_{\text{inj}}} e^{-k_1 t} = A C_{\text{Br}}(t) e^{-k_1 t} \quad (6)$$

where the constant A depends only on the constant of reaction k_1 , the injection time and the initial concentration ratio and is given by:

$$A = \frac{C_{\text{NO}_3}^0}{C_{\text{Br}}^0} \frac{1 - e^{-k_1 t_{\text{inj}}}}{k_1 t_{\text{inj}}}. \quad (7)$$

Eq. (6) can then be used to provide a semi-analytical estimation of the concentrations of the by-products of the chain reaction in Eq. (4). The evolution of all by-products over time was obtained by applying the following reasoning. The concentration evolution of a given by-product with time is the result of competition between its production from previous by-products in the chain, and its consumption. Both terms, production or degradation, are characterized by a reaction constant k_i ($i=2,3,4$) so that a non-homogeneous ordinary

differential equation can be derived for each chemical species as in Eq. (8):

$$\frac{dC_i(t)}{dt} = \text{production} - \text{degradation} = C_{i-1}^{\text{degraded}}(t) - k_i C_i(t) \quad (8)$$

where the general solution is given by

$$C_i(t) = e^{-k_i t} \left(G_i + \int_0^t C_{i-1}^{\text{degraded}}(t') e^{k_i t'} dt' \right) \quad (9)$$

and G_i is an integration constant fixed by the initial concentration of the i -th species. The production term for the i -th species is given by Eq. (9). In accordance with Haggerty et al. (1998), in Eq. (6) we considered the bromide concentration as a dilution coefficient. Therefore the bromide concentration did not have to be integrated over time to find the analytic solution for the chain reaction. We thus defined a relative concentration as:

$$C'_i(t) = \frac{C_i(t)}{C_{\text{Br}}(t)}. \quad (10)$$

By solving the kinetics for this redefined relative concentration, the concentrations could be recovered by multiplying the relative concentration by the bromide concentration. We thus obtained for the different chemical components of the chain:

$$C_{\text{NO}_3}^{\text{degraded}}(t) = k_1 C_{\text{NO}_3}(t) \quad (11)$$

$$C'_{\text{NO}_2}(t) = e^{-k_2 t} \left(G_{\text{NO}_2 i} + \int_0^t k_1 C'_{\text{NO}_3}(t') e^{k_2 t'} dt' \right) \quad (12)$$

$$C_{\text{NO}_2}^{\text{degraded}}(t) = k_2 C_{\text{NO}_2}(t) \quad (13)$$

$$C'_{\text{NO}}(t) = e^{-k_3 t} \left(G_{\text{NO} i} + \int_0^t k_2 C'_{\text{NO}_2}(t') e^{k_3 t'} dt' \right) \quad (14)$$

$$C_{\text{NO}}^{\text{degraded}}(t) = k_3 C_{\text{NO}}(t) \quad (15)$$

$$C'_{\text{N}_2\text{O}}(t) = e^{-k_4 t} \left(G_{\text{N}_2\text{O} i} + \int_0^t k_3 C'_{\text{NO}}(t') e^{k_4 t'} dt' \right). \quad (16)$$

For N_2 , which is the result of the whole denitrification chain, there is no degradation and N_2 is solely dependent on a production term:

$$\begin{aligned} \frac{dC_{\text{N}_2}(t)}{dt} &= \text{production} = C_{\text{N}_2\text{O}}^{\text{degraded}}(t) \rightarrow C_{\text{N}_2}(t) \\ &= \int C_{\text{N}_2\text{O}}^{\text{degraded}}(t') dt' \end{aligned} \quad (17)$$

which leads to

$$C'_{\text{N}_2}(t) = G_{\text{N}_2 i} + \int_0^t (k_4 C'_{\text{N}_2\text{O}}(t')) dt' \quad (18)$$

with

$$C_{\text{N}_2\text{O}}^{\text{degraded}}(t) = k_4 C_{\text{N}_2\text{O}}(t) \quad (19)$$

For the fitting procedure, we adopted a standard approach to estimate the parameters of the model from the field data which minimized the sum of squared residuals, a residual being the difference between an observed value and the fitted value provided by a model. In our case 4 parameters needed to be estimated, namely the 4 reaction constants of the 4 steps in the chain. Each chemical species measured in the chain of reactions is associated with a semi-analytical solution (dependent on the field measurement of bromide concentration). We therefore defined for each solution “u” the estimator S_u defined by:

$$S_u = \sum_i (\text{mass of chemical measured at time } i - \text{mass predicted by the model at time } i)^2 \quad (20)$$

and the global estimator:

$$S = \sum S_u (S_{NO_3} + S_{NO_2} + S_{N_2O} + S_{N_2}) \quad (21)$$

We fitted k_1 by minimizing S_1 . Once k_1 had been fixed, we minimized S_2 to estimate k_2 and continued for the following species. We then assessed the validity of our solution by checking from synthetic data that the total mass balance was maintained throughout the process.

In the following section, we first present results obtained from the laboratory experiments and then a description and modeling of the field experiment.

3. Results

3.1. Laboratory reactor experiments

The initial nitrate concentration of 6.10^{-4} mol/L in the batch reactors decreased between 0 and 815 h (Fig. 2). First order kinetic parameters were obtained from this concentration time course by applying the following equation:

$$C_{NO_3}(t) = C_{0NO_3} e^{-k_1 t} \quad (22)$$

where $C_{NO_3}(t)$ is the nitrate concentration at time t and C_{0NO_3} is the initial concentration. The first order kinetic parameter, k_1 , obtained from the experimental data is $k_1 = 0.0008 \text{ h}^{-1}$. This degradation represents the first step of the reaction (4) and all the NO_3^- that has been degraded may be considered as degraded to NO_2^- . During its production, the NO_2^- is also being degraded to NO. This can be modeled according to a first order reaction rate as in the following equation:

$$C_{NO_2}(t) = e^{-k_2 t} \left(G_{NO_2} + \int_0^t k_1 C_{NO_2\text{-prod}}(t') e^{k_2 t'} dt' \right) \quad (23)$$

where G_{NO_2} is the initial concentration of nitrites, $C_{NO_2\text{-prod}}$ corresponds to the NO_3^- reduced and k_2 is the first order kinetic parameter. The parameter obtained ($k_2 = 0.0059 \text{ h}^{-1}$) for NO_2^- was higher than for NO_3^- indicating that NO_2^- was degraded more rapidly than NO_3^- . However, this degradation did not occur fast enough to prevent an accumulation of NO_2^- . These data were then used 1) to compare the behaviors of nitrate and nitrite evolution with the field experiment and 2) as reference kinetic parameters because no published data are available for this chain reaction.

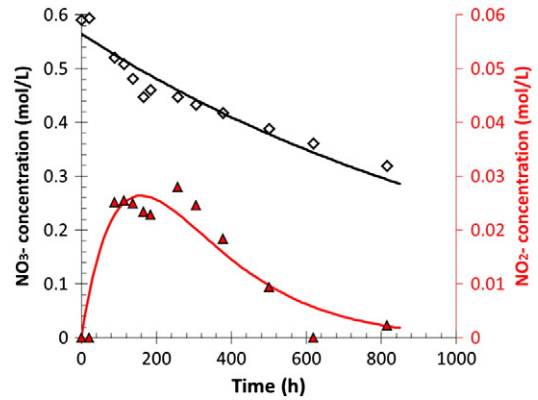


Fig. 2. Evolution with time of nitrate (black) and nitrite (red) concentrations in batch reactors.

3.2. Push–pull breakthrough curves

In the following section the results of the push–pull experiment are discussed and the developed model is used to obtain first order kinetic parameters for the complete chain reaction.

3.2.1. Data analysis

The breakthrough curves obtained when pumping back the tracers are shown in Fig. 3. Drawdown (Fig. 3a), relative tracer concentrations (Fig. 3b) and concentrations of by-products (Fig. 3c) are plotted against relative time since injection. In these plots, time 0 to 70 min corresponds to the injection phase (tracer from 0 to 16 min and chaser from 16 to 70 min), and time 70 to 140 min corresponds to resting time. Since the pump was located at 40 m depth in the borehole whereas the injection was carried out at 64 m in front of the fracture zone, a volume of water in the borehole located between the fractured zone and the pump needed to be removed before water in the aquifer could be extracted and sampled. Note that part of this water volume might also have been slightly mixed with tracer solution during the injection phase. Thus the volume pumped between 140 and 215 min corresponded to the volume of water that remained in the borehole. This volume of about 1.25 m^3 , was pumped for 75 min and corresponded to i) the volume between the bottom of the fractured zone and the pump plus, and ii) the wellbore storage implied by the observed rapid drawdown in the well during this period. Later times, from 215 to 720 min, correspond to tracer recovery from the aquifer. The relative concentration during the recovery phase was very low: $C/C_0 = 0.05$. This was because the tracer was injected in a large borehole (22 cm diameter) at a low flow rate due to the poor permeability of the medium. Therefore this low relative concentration was mainly derived from the injection process but did not affect the parameter estimations from the model.

3.2.1.1. Reactivity within the borehole. From 140 to 215 min, some tracer was detected in the pumped water (Fig. 3) although the pumped volume corresponded to the volume of water present in the borehole prior to water sampling from the aquifer. This implies that some partial mixing of the tracer mass occurred within the borehole. Moreover, during this phase, the

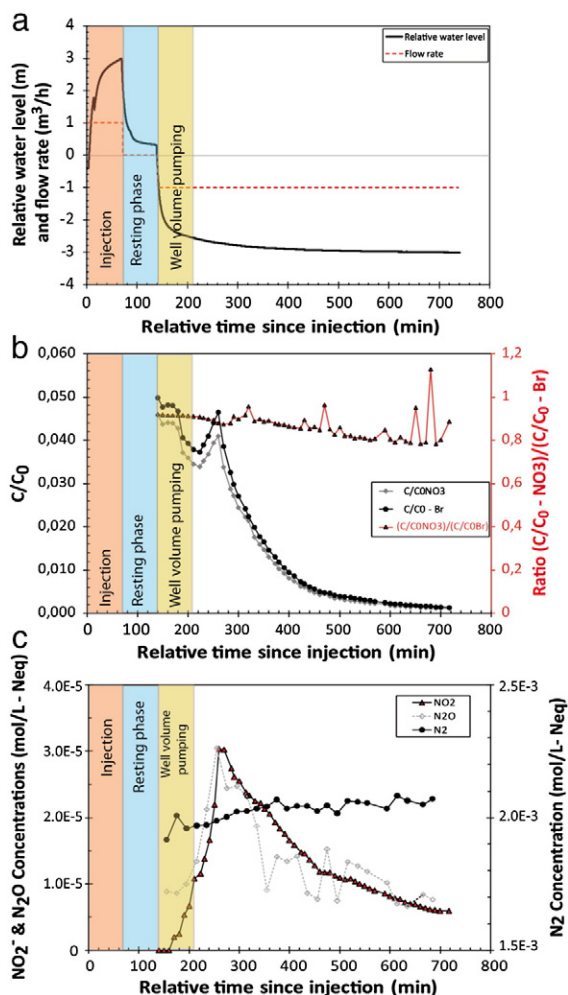


Fig. 3. Results of the push–pull test experiment: a) piezometric head evolution with time highlighting the different phases of the push–pull test; b) normalized breakthrough curves for nitrates and bromides; c) breakthrough curves for the reaction by-products NO_2^- , N_2O , and N_2 .

ratio $C_{\text{NO}_3(t)}/C_{\text{ONO}_3}/C_{\text{Br}(t)}/C_{\text{OBr}}$ was less than 1 implying that NO_3^- reduction occurred within the borehole. This reaction may be related to Fe^{2+} oxidation as predicted by Eq. (2) since Fe^{2+} was present in the borehole water (5 mg/L) and considerable bacterial development related to iron oxides had been observed in nearby piezometers. It should be noted however that this reaction, which represented 28% of the total NO_3^- reduced during the whole experiment, was characterized by the absence of NO_2^- production.

3.2.1.2. Reactivity within the aquifer. No organic carbon was detected in the water before or during the test (<0.04 mg/L), implying that the observed reaction was autotrophic denitrification. Abiotic denitrification is considered to be very slow (Weber et al., 2001) which means that it cannot be observed in a single day experiment in natural systems. Moreover bacteria are always present in natural hydrosystems and considerable biofilm development had been observed in another borehole

close-by. Thus, it seems reasonable to consider this as a microbially-mediated reaction. An autotrophic reaction due to pyrite-bearing fractures had been previously observed in the Ploemeur site (Tarits et al., 2006) following Eqs. (2) and (3). A slight increase of SO_4^{2-} from 33 mg/L to 50 mg/L was also observed during the experiment which further suggests an autotrophic reaction. Nevertheless, this increase of SO_4^{2-} cannot be fully correlated with the observed NO_3^- reduction and may be partially related to mixing. However, even when such a denitrification reaction occurs, the stoichiometric ratios are often not fully observed due to mixing and precipitation (Pauwels et al., 1998; Zhang et al., 2012). The concentration of Fe^{2+} also suggests the possibility of the reaction defined in Eq. (3). We thus considered in the following that the observed autotrophic reaction was ruled by Eqs. (2) and (3).

For times longer than 215 min, which corresponded to water extracted from the aquifer, the $C_{\text{NO}_3(t)}/C_{\text{ONO}_3}$ and $C_{\text{Br}(t)}/C_{\text{OBr}}$ ratios were relatively low due to dilution during the injection phase (Fig. 3a) but the $C_{\text{NO}_3(t)}/C_{\text{ONO}_3}/C_{\text{Br}(t)}/C_{\text{OBr}}$ ratio remained below 1 which indicated NO_3^- reduction (Fig. 3b). This exhibited a linear decrease with time. Extrapolation of this slope to an early stage of the experiment led to a ratio $C_{\text{NO}_3(t)}/C_{\text{ONO}_3}/C_{\text{Br}(t)}/C_{\text{OBr}}$ of 1 (no NO_3^- reduction) at time 0 min. This shows that the reaction started at the beginning of the experiment without a biological lag phase, which is consistent with the reactivity observed within the borehole during continuous monitoring under ambient conditions. This possible lag phase may typically correspond to the adaptation time required for a microbial population to adapt to a new component before consuming it (e.g.: production of new enzymes) (Marazioti et al., 2003). Thus the microbial population appears to be already adapted and did not need a lag time before starting NO_3^- reduction.

Fig. 3c displays the reaction by-products and shows that the production of NO_2^- and N_2O is clearly related to the NO_3^- concentration. For both products, the peaks are located at the same time as those of NO_3^- and Br^- . The breakthrough curves of these by-products confirm the occurrence of the reactivity observed from the difference between the $C_{\text{NO}_3(t)}/C_{\text{ONO}_3}$ and $C_{\text{Br}(t)}/C_{\text{OBr}}$ ratios.

The cumulative NO_3^- quantity reduced, the NO_3^- reduced to NO or N_2 (total NO_3^- reduced minus NO_2^- and N_2O produced), the NO_2^- produced and the N_2O produced are shown in Fig. 4. The total injected NO_3^- mass in the geological medium was 4.6 mol. The total quantity of NO_3^- reduced was 0.45 mol, i.e., only 9.8% of the injected quantity. Moreover, the denitrification reaction was incomplete and only part of the reduced NO_3^- was reduced to N_2 . About 0.13 mol of NO_2^- (2.7% of the injected mass and 29% of the reduced NO_3^-) and 0.096 mol of N_2O (0.048 mol-Neq) was produced (1% of the injected quantity and 8% of the reduced NO_3^-). Those results are summarized in Table 1.

3.2.2. Modeling results

The cumulative mass of NO_3^- reduced and by-products are plotted in Fig. 5 with the semi analytical solutions for the different elements. As explained, the early times of the breakthrough curves for NO_3^- and Br^- (from 140 to 215 min after injection) are indicative of reactivity occurring in the borehole (9 data points). To satisfy data integration needs, 9 artificial data points were created, for Br^- only, between pumping time 0 and the peak. These data were created by

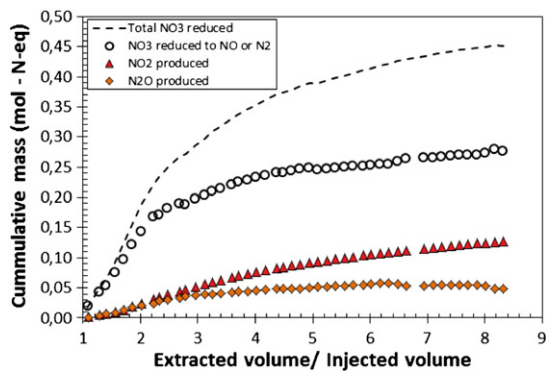


Fig. 4. Cumulative mass of nitrates reduced and reaction by-products produced.

fitting the peak location and magnitude to the analytical solution. As our fitting procedure was carried out on i) peak location and ii) the decay slope, this procedure had little effect and acted only on the initial slope of the concentration increase and the magnitude of the breakthrough curve. Therefore a slight difference was observed between the cumulative mass of NO_3^- given in Figs. 4 and 5. This difference corresponds to the 28% reduction calculated in Section 3.2.1.1. Other elements were not affected. The parameters used and the estimated reaction constants are given in Table 2.

4. Discussion

4.1. Model limitations

The main factors influencing the estimation of reaction coefficients were breakthrough tailing and peak locations. The decay slope in the case of NO_3^- is only dependent on the k_1 value whereas the NO_2^- decay slope integrates both k_1 and k_2 . The NO decay slope integrates k_1 , k_2 and k_3 whereas N_2O integrates k_1 , k_2 , k_3 and k_4 . These parameters can therefore be easily determined in the case of k_1 as nitrate is the only element involved (Haggerty et al., 1998) but due to integration of the previous parameters, the uncertainty increases along the chain reaction and the parameters for the end of the chain reaction are therefore much less well-defined. The last parameter determination should be considered as a relative estimate with the greatest uncertainty. In summary, a variation of k_4 has almost no influence on the modeled concentration of N_2O whereas the entire chain reaction is much more influenced by the choice of k_1 which is the principal parameter of the chain reaction.

Table 1
Mass balance calculations.

Species	Injected concentration (mol/L)	Initial concentration in the medium (mol/L)	Maximum concentration (mol/L)	Reduced/produced mass (mol-Neq)
NO_3^-	$3.10 \cdot 10^{-2}$	0	$1.40 \cdot 10^{-3}$	0.45 – reduced
NO_2^-	0	0	$3.02 \cdot 10^{-5}$	0.13 – produced
N_2O	0	$8.10 \cdot 10^{-6}$	$3.04 \cdot 10^{-5}$	0.048 – produced
N_2	0	$1.90 \cdot 10^{-3}$	$2.00 \cdot 10^{-3}$	0.4 – produced

4.2. Modeled kinetic parameters

The measured versus modeled cumulative masses (Fig. 5) showed very good agreement. The modeled masses followed the global behavior of the experiment. The constant k_1 derived from the model was similar to that obtained from the solution of Haggerty et al. (1998). The deviations between experimental data and the model can be explained in various ways. First, the reaction rate at each step may evolve with time as it is related to microbial development. As NO_3^- reduction begins with the injection the indigenous populations seem to already be adapted and able to reduce nitrate immediately. However as observed in various studies (Maraziotti et al., 2003), the next step, NO_2^- reduction, may exhibit a lag phase due to population adaptation since low or negligible NO_2^- concentrations are usually present in the geological medium. This adaptation phenomenon is also true for the other steps of the chain reaction and may explain the slight differences between predicted and observed NO_2^- concentrations (Fig. 5). A second effect which was not taken into account is related to the heterogeneity of the medium. As the injected solution flows through heterogeneous media, it experiences different flow velocities depending on the fracture aperture. This may locally change both the reaction rates and microbial population developments since the contact surface and residence time in each flow path may be different. Nevertheless, the good agreement between the experimental data and the model shows that the proposed chain reaction can be used with success as a first-order model of autotrophic denitrification.

For both experiments, the estimated kinetic parameters (k_i) were coherent. For both experiments the k_2 values were higher for NO_2^- ($k_2 = 0.5 \text{ h}^{-1}$) than for NO_3^- ($k_1 = 0.022 \text{ h}^{-1}$). This more rapid degradation has been observed by various authors in laboratory experiments. The obtained value of $k_1 = 0.022 \text{ h}^{-1}$ for field experiments is nevertheless within the lowest range of values presented in McGuire et al. (2002) and references herein. However the reaction rates for the heterotrophic reactions assessed by McGuire et al. (2002) are expected to be greater than for our autotrophic reaction. For the by-products, no studies have been found in the literature to allow comparison, so the absolute values of the parameters cannot be further compared.

4.3. In situ/laboratory experiments comparison

The kinetic parameters derived from batch laboratory experiments and the push–pull field experiment, did not lead to the same first order reaction rates. Faster rates were observed in the field ($k_1 = 0.0035 \text{ h}^{-1}$ in the case of laboratory experiments and 0.023 h^{-1} in the case of the field experiment). For NO_2^- the coefficients were $k_2 = 0.59 \text{ h}^{-1}$ for the field experiment and $k_2 = 0.0081 \text{ h}^{-1}$ for the batch experiment, leading to an even larger difference between the laboratory experiments and push–pull tracer tests. Discrepancies between laboratory and field experiments are common due to differences in conditions such as fracture coating minerals, existing bacterial biofilms and/or redox conditions and the water rock interaction ratio. Although field measurements may also present some variability due to chemical heterogeneity (McGuire et al., 2002; Schroth et al., 1998) and flow heterogeneity, they confirm the need for in situ field measurements to assess the reactivity of natural systems.

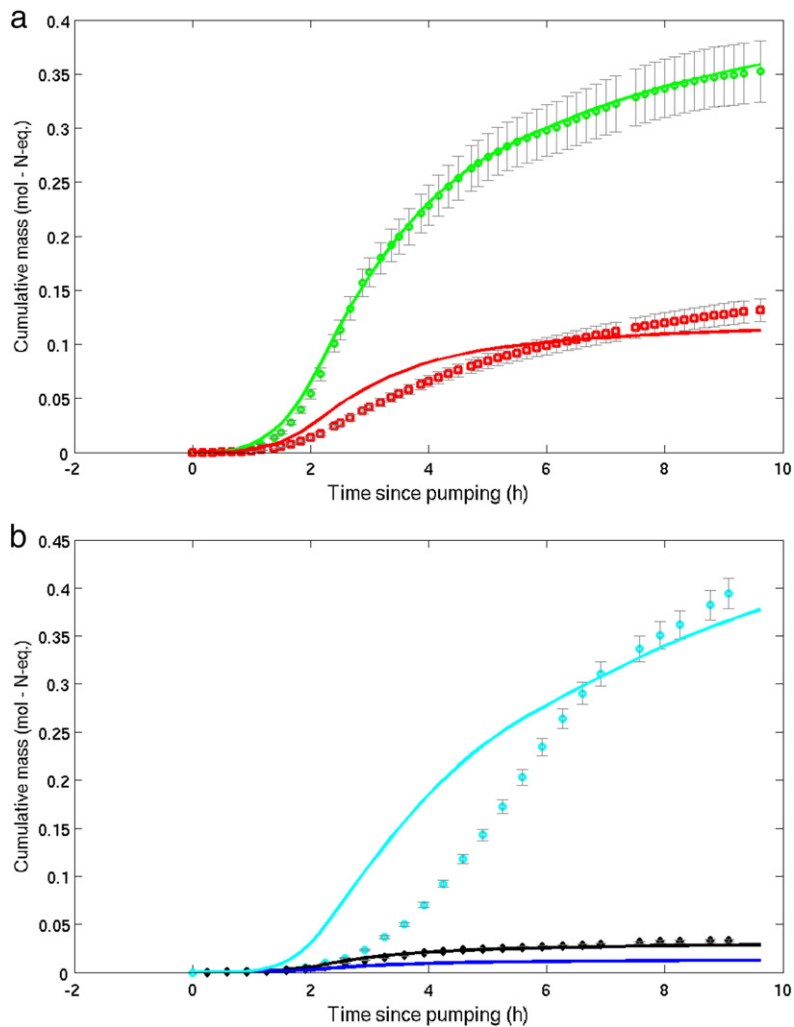


Fig. 5. Cumulative mass of the total reduced NO_3^- (a-green); produced NO_2^- (a-red); produced N_2O (b-black) and N_2 (b-cyan). Curves represent model results for each compound. The blue line (b) represents the estimated NO mass production. The dashed line represents theoretical N_2 production. Error bars represent the analytical error.

4.4. By-product production

In both experiments the amount of NO_3^- reduced was relatively limited (10% in the case of push–pull and 50% in the case of the laboratory reactor). However, the formation of by-products was well quantified and indicated an incomplete reaction. When subtracted from the total amount of NO_3^- reduced, it was apparent that only 0.28 mol of NO_3^- was reduced to N_2 or NO (curve labeled NO_3^- reduced to NO or N_2 in Fig. 4). The

Table 2

Model parameters.

Known parameters			Estimated reaction constants		
Parameter	Value	Unit	Parameter	Value	Unit
C_{NO_3}	0.031	mol/L	k_1	0.023	h^{-1}
C_{OBr}	0.017	mol/L	k_2	0.59	h^{-1}
Q	1090	L/h	k_3	16	h^{-1}
T_{inj}	15	min	k_4	5.5	h^{-1}

proportion of N_2O produced was higher than observed in other experiments (Laverman et al., 2010; Silvennoinen et al., 2008). For example, Laverman et al. (2010) reported N_2O produced to NO_3^- reduced ratios of 0.06% as compared to 8% in our experiments. Although autotrophic denitrification has been observed to produce a higher rate of N_2O per NO_3^- consumed (Weymann et al., 2010), our ratios are larger than those previously measured. However our model of the dependency of the different by-products of a chain reaction shows that the ratios of by-product formation over NO_3^- reduced were not constant and evolved with time. The observed ratios were therefore dependent on the duration of the experiments. Moreover, the reaction kinetics may vary with the location, the microbial community (Holtan-Hartwig et al., 2000) and temperature (Holtan-Hartwig et al., 2002). The observed difference is difficult to interpret and indicates that more data are required to better characterize the field dynamics of denitrification. For this purpose, it could be interesting to carry out reactive push–pull tests with different

injections or resting durations. To increase the accuracy of the measurements it might also be useful to perform nitrogen isotopic analyses as done by previous authors (Fukada et al., 2003; Mariotti et al., 1988; Otero et al., 2009; Pauwels et al., 2010; Zhang et al., 2012). As the microbial reaction fractionates the nitrogen isotopes and the local isotopic ratios are relatively well known (Pauwels et al., 2010) this would allow better quantification of the extent of denitrification.

5. Conclusions

The model developed for chain reaction interpretation provides a comprehensive framework for assessing a chain reaction via push–pull tests. It allows derivation of the kinetic parameters and a better understanding of the interactions between different kinetic parameters. As expected the estimated constant k_1 for the transformation of NO_3^- to NO_2^- is the main parameter of the model. We were able to highlight the fact that biogeochemical reactions such as denitrification may be efficiently modeled as a chain reaction. This model can easily be used to model other chain reactions as it does not require any direct information about the aquifer properties (geometry, porosity, permeability or dispersivity).

The push–pull test, which was carried out in a fractured crystalline aquifer to test the model, was also compared to batch experiments performed on rock and water samples from the site. This field experiment demonstrated the reliability of using push–pull tests to assess the autotrophic denitrification reaction including by-product formation. The NO_3^- reduction coefficient rates determined from laboratory experiments revealed lower coefficients than the field estimates. This study provides a first set of coefficients for the complete reaction kinetics which was not available previously. Further experiments, possibly using nitrogen isotopes, could be carried out to assess the evolution of the reaction rate with time and its dependency on flow conditions. The role of the heterogeneity of the medium at the field scale could also be further investigated.

Acknowledgments

The French National Research Agency ANR is acknowledged for its financial funding through the MOHINI project (ANR-07-VULN-008) as well as the European Union RDF INTERREG IVA France (Channel)-England program through the CLIMAWAT project. The field data investigations were also supported by the network of hydrogeological research sites H+ (SOERE H+). The authors are also grateful to Dr. Greg B. Davis and anonymous reviewers for their valuable and constructive comments.

References

- Addy, K., Kellogg, D.Q., Gold, A.J., Groffman, P.M., Ferendo, G., Sawyer, C., 2002. In situ push–pull method to determine ground water denitrification in riparian zones. *Journal of Environmental Quality* 31 (3), 1017–1024.
- Altman, S.J., Meigs, L.C., Jones, T.L., McKenna, S.A., 2002. Controls of mass recovery rates in single-well injection-withdrawal tracer tests with a single-porosity, heterogeneous conceptualization. *Water Resources Research* 38 (7), 1125.
- Amirbahman, A., Schonenberger, R., Furrer, G., Zobrist, J., 2003. Experimental study and steady-state simulation of biogeochemical processes in laboratory columns with aquifer material. *Journal of Contaminant Hydrology* 64 (3–4), 169–190.
- Aquilina, L., Vergnaud-Ayraud, V., Labasque, T., Bour, O., Molenat, J., Ruiz, L., de Montety, V., De Ridder, J., Roques, C., Longuevergne, L., 2012. Nitrate dynamics in agricultural catchments deduced from groundwater dating and long-term nitrate monitoring in surface- and groundwaters. *The Science of the Total Environment* 435–436, 167–178.
- Bauer, P., Attinger, S., Kinzelbach, W., 2001. Transport of a decay chain in homogeneous porous media: analytical solutions. *Journal of Contaminant Hydrology* 49 (3–4), 217–239.
- Becker, M.W., Shapiro, A.M., 2003. Interpreting tracer breakthrough tailing from different forced-gradient tracer experiment configurations in fractured bedrock. *Water Resources Research* 39 (1), 1024.
- Betlach, M.R., Tiedje, J.M., 1981. Kinetic explanation for accumulation of nitrite, nitric oxide, and nitrous oxide during bacterial denitrification. *Applied and Environmental Microbiology* 42 (6), 1074–1084.
- Cozzarelli, I.M., Herman, J.S., Baedecker, M.J., Fischer, J.M., 1999. Geochemical heterogeneity of a gasoline-contaminated aquifer. *Journal of Contaminant Hydrology* 40 (3), 261–284.
- de Dreuzy, J.R., Bodin, J., Le Grand, H., Davy, P., Boulanger, D., Battais, A., Bour, O., Guze, P., Porel, G., 2006. Groundwater database for site and processes studies. *Ground Water* 44 (5), 743–748.
- Dentz, M., Le Borgne, T., Englert, A., Bijeljic, B., 2011. Mixing, spreading and reaction in heterogeneous media: a brief review. *Journal of Contaminant Hydrology* 120–21, 1–17.
- Fukada, T., Hiscock, K.M., Dennis, P.F., Grischek, T., 2003. A dual isotope approach to identify denitrification in groundwater at a river-bank infiltration site. *Water Research* 37, 3070–3078.
- Guze, P., Le Borgne, T., Leprovost, R., Lods, G., Poidras, T., Pezard, P., 2008. Non-Fickian dispersion in porous media: 1. Multiscale measurements using single-well injection withdrawal tracer tests. *Water Resources Research* 44 (6), W06426.
- Haggerty, R., Schroth, M.H., Istok, J.D., 1998. Simplified method of “push–pull” test data analysis for determining in situ reaction rate coefficients. *Ground Water* 36 (2), 314–324.
- Haggerty, R., Fleming, S.W., Meigs, L.C., McKenna, S.A., 2001. Tracer tests in a fractured dolomite 2. Analysis of mass transfer in single-well injection-withdrawal tests. *Water Resources Research* 37 (5), 1129–1142.
- Hiscock, K.M., Bateman, A.S., Muhlherr, I.H., Fukada, T., Dennis, P.F., 2003. Indirect emissions of nitrous oxide from regional aquifers in the United Kingdom. *Environmental Science & Technology* 37 (16), 3507–3512.
- Holtan-Hartwig, L., Dörsh, P., Bakken, L.R., 2000. Comparison of denitrifying communities in organic soils: kinetics of NO_3^- and N_2O reduction. *Soil Biology and Biochemistry* 32, 833–843.
- Holtan-Hartwig, L., Dörsh, P., Bakken, L.R., 2002. Low temperature control of soil denitrifying communities: kinetics of N_2O production and reduction. *Soil Biology and Biochemistry* 34, 1797–1806.
- Istok, J.D., Humphrey, M.D., Schroth, M.H., Hyman, M.R., O'Reilly, K.T., 1997. Single-well, “push–pull” test for in situ determination of microbial activities. *Ground Water* 35 (4), 619–631.
- Jury, W.A., Roth, K., 1990. *Transfer Function and Solute Movement Through Soil*. Birkhauser Verlag, Basel.
- Kim, Y., Kim, J.H., Son, B.H., Oa, S.W., 2005. A single well push–pull test method for in situ determination of denitrification rates in a nitrate-contaminated groundwater aquifer. *Water Science and Technology* 52 (8), 77–86.
- Knowles, R., 1982. Denitrification. *Microbiological Reviews* 46 (1), 43–70.
- Korom, S.F., 1992. Natural denitrification in the saturated zone – a review. *Water Resources Research* 28 (6), 1657–1668.
- Laverman, A.M., Garnier, J.A., Mounier, E.M., Roose-Amsaleg, C.L., 2010. Nitrous oxide production kinetics during nitrate reduction in river sediments. *Water Research* 44 (6), 1753–1764.
- Le Borgne, T., Guze, P., 2008. Non-Fickian dispersion in porous media: 2. Model validation from measurements at different scales. *Water Resources Research* 44 (6), 10.
- Le Borgne, T., Bour, O., Paillet, F.L., Caudal, J.P., 2006. Assessment of preferential flow path connectivity, and hydraulic properties at single-borehole and cross-borehole scales in a fractured aquifer. *Journal of Hydrology* 328, 347–359.
- Le Borgne, T., Bour, O., Riley, M.S., Guze, P., Pezard, P., Belghoul, A., Lods, G., Le Provost, R., Greswell, R.B., Ellis, P.A., Isakov, E., Last, B.J., 2007. Comparison of alternative methodologies for identifying and characterizing preferential flow paths in heterogeneous aquifers. *Journal of Hydrology* 345 (3), 134–148.
- Leray, S., de Dreuzy, J.-R., Bour, O., Labasque, T., Aquilina, L., 2012. Contribution of age data to the characterization of complex aquifers. *Journal of Hydrology* 464, 54–68.
- Marazioti, C., Kornaros, M., Lyberatos, G., 2003. Kinetic modeling of a mixed culture of *Pseudomonas denitrificans* and *Bacillus subtilis* under aerobic and anoxic operating conditions. *Water Research* 37 (6), 1239–1251.
- Mariotti, A., 1986. Denitrification in groundwaters, principles and methods for its identification – a review. *Journal of Hydrology* 88, 1–23.

- Mariotti, A., Landreau, A., Simon, B., 1988. 15 N isotope biogeochemistry and natural denitrification process in groundwater: application to the chalk aquifer of northern France. *Geochimica et Cosmochimica Acta* 52, 1869–1878.
- McAllister, P.M., Chiang, C.Y., 1994. A practical approach to evaluating natural attenuation of contaminant in groundwater. *Ground Water Monitoring and Remediation* 14 (2), 161–173.
- McGuire, J.T., Long, D.T., Klug, M.J., Haack, S.K., Hyndman, D.W., 2002. Evaluating behavior of oxygen, nitrate, and sulfate during recharge and quantifying reduction rates in a contaminated aquifer. *Environmental Science & Technology* 36 (12), 2693–2700.
- Meigs, L.C., Beauheim, R.L., 2001. Tracer tests in a fractured dolomite: 1. Experimental design and observed tracer recoveries. *Water Resources Research* 37 (5), 1113–1128.
- Miotliński, K., 2008. Coupled reactive transport modeling of redox processes in a nitrate-polluted sandy aquifer. *Aquatic Geochemistry* 14 (2), 117–131.
- Molz, F.J., Boman, G.K., Young, S.C., Waldrop, W.R., 1994. Borehole flowmeters – field application and data-analysis. *Journal of Hydrology* 163, 347–371.
- Mosier, A., Kroeze, C., Nevison, C., Oenema, O., Seitzinger, S., van Cleemput, O., 1998. Closing the global N₂O budget: nitrous oxide emissions through the agricultural nitrogen cycle – OECD/IPCC/IEA phase II development of IPCC guidelines for national greenhouse gas inventory methodology. *Nutrient Cycling in Agroecosystems* 52, 225–248.
- Muhlherr, I.H., Hiscock, K.M., 1998. Nitrous oxide production and consumption in British limestone aquifers. *Journal of Hydrology* 211, 126–139.
- Otero, N., Torrento, C., Soler, A., Mencio, A., Mas-Pla, J., 2009. Monitoring groundwater nitrate attenuation in a regional system coupling hydrogeology with multi-isotopic methods: the case of Plana de Vic (Osona, Spain). *Agriculture, Ecosystems and Environment* 133, 103–113.
- Paillet, F.L., 1998. Flow modeling and permeability estimation using borehole flow logs in heterogeneous fractured formations. *Water Resources Research* 34 (5), 997–1010.
- Pauwels, H., Kloppmann, W., Foucher, J.C., Martelat, A., Fritsche, V., 1998. Field tracer test for denitrification in a pyrite-bearing schist aquifer. *Applied Geochemistry* 13 (6), 767–778.
- Pauwels, H., Ayraud-Vergnaud, V., Aquilina, L., Molenat, J., 2010. The fate of nitrogen and sulfur in hard-rock aquifers as shown by sulfate-isotope tracing. *Applied Geochemistry* 25 (1), 105–115.
- Philippot, L., Cuhel, J., Saby, N.P.A., Cheneby, D., Chmukova, A., Bru, D., Arrouays, D., Martin Laurent, F., Simek, M., 2009. Mapping field-scale spatial patterns of size and activity of the denitrifier community. *Environmental Microbiology* 11 (6), 1518–1526.
- Postma, D., Appelo, C.A.J., 2000. Reduction of Mn-oxides by ferrous iron in a flow system: column experiment and reactive transport modeling. *Geochimica Et Cosmochimica Acta* 64 (7), 1237–1247.
- Postma, D., Boesen, C., Kristiansen, H., Larsen, F., 1991. Nitrate reduction in an unconfined sandy aquifer – water chemistry, reduction processes, and geochemical modeling. *Water Resources Research* 27 (8), 2027–2045.
- Quezada, C.R., Clement, T.P., Lee, K.K., 2004. Generalized solution to multi-dimensional multi-species transport equations coupled with a first-order reaction network involving distinct retardation factors. *Advances in Water Resources* 27 (5), 507–521.
- Ruelleu, S., Moreau, F., Bour, O., Gapais, D., Martelet, G., 2010. Impact of gently dipping discontinuities on basement aquifer recharge: an example from Ploemeur (Brittany, France). *Journal of Applied Geophysics* 70 (2), 161–168.
- Schroth, M.H., Istok, J.D., Conner, G.T., Hyman, M.R., Haggerty, R., O'Reilly, K.T., 1998. Spatial variability in situ aerobic respiration and denitrification rates in a petroleum-contaminated aquifer. *Ground Water* 36 (6), 924–937.
- Silvennoinen, H., Liikanen, A., Torssonen, J., Stange, C.F., Martikainen, P.J., 2008. Denitrification and nitrous oxide effluxes in boreal, eutrophic river sediments under increasing nitrate load: a laboratory microcosm study. *Biogeochemistry* 91 (2), 105–116.
- Tarits, C., Aquilina, L., Ayraud, V., Pauwels, H., Davy, P., Touchard, F., Bour, O., 2006. Oxido-reduction sequence related to flux variations of groundwater from a fractured basement aquifer (Ploemeur area, France). *Applied Geochemistry* 21 (1), 29–47.
- Touchard, F., 1999. Caractérisation hydrogéologique d'un aquifère en socle fracturé - Site de Ploemeur Morbihan. Université de Rennes 1.
- Tsang, Y.W., 1995. Study of alternative tracer tests in characterizing transport in fractured rocks. *Geophysical Research Letters* 22 (11), 1421–1424.
- Vandenbohede, A., Louwyck, A., Lebbe, L., 2008. Identification and reliability of microbial aerobic respiration and denitrification kinetics using a single-well push-pull field test. *Journal of Contaminant Hydrology* 95 (1–2), 42–56.
- Vongunten, U., Zobrist, J., 1993. Biogeochemical changes in groundwater-infiltration systems – column studies. *Geochimica Et Cosmochimica Acta* 57 (16), 3895–3906.
- Weber, K.A., Picardal, F.W., Roden, E.E., 2001. Microbially catalyzed nitrate-dependent oxidation of biogenic solid-phase Fe(II) compounds. *Environmental Science & Technology* 35 (8), 1644–1650.
- Weymann, D., Well, R., Flessa, H., von der Heide, C., Deurer, M., Meyer, K., Konrad, C., Walther, W., 2008. Groundwater N₂O emission factors of nitrate-contaminated aquifers as derived from denitrification progress and N₂O accumulation. *Biogeosciences* 5 (5), 1215–1226.
- Weymann, D., Geistlinger, H., Well, R., von der Heide, C., Flessa, H., 2010. Kinetics of N₂O production and reduction in a nitrate-contaminated aquifer inferred from laboratory incubation experiments. *Biogeosciences* 7 (6), 1953–1972.
- Zhang, Y., Slomp, C.P., Broers, H.P., Passier, H.F., Van Cappellen, P., 2009. Denitrification coupled to pyrite oxidation and changes in groundwater quality in a shallow sandy aquifer. *Geochimica et Cosmochimica Acta* 73, 6716–6726.
- Zhang, Y.C., Slomp, C.P., Broers, H.P., Bostick, B., Passier, H.F., Böttcher, M.E., Omeregie, E.O., Lloyd, J.R., Polyá, D.A., Van Cappellen, P., 2012. Isotopic and microbiological signatures of pyrite-driven denitrification in a sandy aquifer. *Chemical Geology* 300–301, 123–132.